Physisorption of Molecular Hydrogen on Polycyclic Aromatic Hydrocarbons: A Theoretical Study

Fabien Tran, Jacques Weber, and Tomasz A. Wesołowski*

Department of Physical Chemistry, University of Geneva, 30 quai Ernest-Ansermet, CH-1211 Geneva 4, Switzerland

Frikia Cheikh,[†,‡] Yves Ellinger,[†] and Françoise Pauzat[†]

Laboratoire d'Etude Théorique des Milieux Extrêmes, Université de Nice-Sophia Antipolis et Observatoire de la Côte d'Azur, Parc Valrose, 06108 Nice, France, and Laboratoire de Chimie Théorique, Institut de Chimie, USTHB, B.P. 32 El Alia, 16111 Bab Ezzouar, Alger, Algérie

Received: November 27, 2001; In Final Form: April 23, 2002

The repartition of molecular hydrogen in space, and its depletion on solid particles in particular, is an important question of modern astrophysics. In this paper, we report a theoretical study of the physisorption of molecular hydrogen, H_2, on a major component of the interstellar dust known as polycyclic aromatic hydrocarbons (PAHs). Two different density functional theory approaches were used: (i) the conventional Kohn−Sham theory and (ii) the subsystem-based approach (Kohn−Sham equations with constrained electron density, KSCED) developed in our group. The approximate exchange-correlation energy functional applied in all calculations and the nonadditive kinetic-energy functional needed in KSCED have a generalized gradient approximation form and were chosen on the basis of our previous studies. The results of both approaches show similar trends: weak dependence of the calculated interaction energies on the size of the PAH and negligible effect of the complexation of two PAH molecules on the adsorption of molecular hydrogen. The KSCED interaction energy calculated for the largest considered PAH (ovalene), amounting to 1.27 kcal/mol, is in excellent agreement with experimental estimates ranging from 1.1 to 1.2 kcal/mol, whereas the one derived from supermolecular Kohn−Sham calculations is underestimated by more than 50%. This result is in line with our previous studies, which showed that the generalized gradient approximation applied within the KSCED framework leads to interaction energies of weakly bound complexes that are superior to the corresponding results of supermolecular Kohn−Sham calculations.

I. Introduction

Hydrogen, in all its forms (atom, molecule, cluster, or solid; neutral or ionic), occupies an important place in astrophysics (for a recent survey, see ref 1). Molecular hydrogen, H_2, is the first neutral molecule to be formed and is the most abundant molecule in the universe. Despite the fact that many studies have been devoted to this fundamental molecule, a number of problems are still unsolved. It is now well-established, for example, that the chemistry of H_2 cannot be understood without taking into account the gas/surface interactions: this molecule, simply, cannot be formed otherwise. In a general sense, space chemistry can no longer be limited to gas-phase reactivity but must consider reactions at surfaces (ices, silicates, crystalline or amorphous carbon, etc.). Among the various surfaces available, graphite has already been proposed in 1976 as one of the most effective in the production of H_2,[2] and recent theoretical studies have been devoted to study the underlying mechanism (see refs 3−11 and Sidis et al. in ref 1). Graphite has also been proposed as a possible agent in the depletion of transition metals.[12] The presence of polycyclic aromatic hydrocarbons (PAHs) in the interstellar medium (for comprehensive surveys, see refs 13 and 14 and references therein), which is now well-admitted in the astrophysical community as a major hypothesis for interpreting the so-called unidentified infrared emission (UIR bands),[15,16] raises the question of their possible role in hydrogen chemistry. In this context, the interaction of molecular hydrogen with graphite surfaces or free-flyer PAHs is of utmost importance because its sticking may strongly affect the gas-phase abundance of H_2 in a large variety of astrophysical objects.

In fact, very little is known about depletion of molecules at carbonaceous surfaces. Because the size of the surface that should be considered in the study of grain properties must extend over several benzene rings, very accurate correlated ab initio methods such as configuration interaction or coupled cluster cannot be effectively applied for that purpose, although they could be very useful for calibration on smaller complexes.

For that reason, we turned to density functional theory (DFT)[17,18] as an alternative, keeping in mind that describing the energetics of weakly bound complexes faces serious practical and conceptual difficulties (for a brief review, see ref 19). Although the exact exchange-correlation energy functional defined in Kohn−Sham theory[20] should lead to the exact description of such complexes, the approximate functionals developed so far suffer from serious flaws. Neither local density approximation (LDA) nor semilocal generalized gradient approximation (GGA) applied in a hypothetical case of two

[†] Université de Nice-Sophia Antipolis et Observatoire de la Côte d'Azur.
[‡] USTHB.

10.1021/jp015590h CCC: $22.00
Published on Web 07/27/2002

nonoverlapping spherical electron densities can lead to any attraction. Therefore, the correct description of the asymptotic behavior of the interaction energy (proportional to R^{-6}) arising from London dispersion forces is beyond reach of currently used local and semilocal approximations. Moreover, the overlap between the electron densities of molecules forming a van der Waals complex is usually very small at the equilibrium geometry, making the Kohn−Sham interaction energies strongly dependent on the choice of the applied approximate GGA functional as originally demonstrated and underlined in our previous work[21] and in the paper of Yang and co-workers.[22] As a result of these flaws, applying such approximate exchange-correlation energy functionals, which proved to be very reliable in describing covalently bound systems, to weakly bound complexes leads to unreliable results as illustrated by many examples (see also refs 23 and 24).

Our previous work[21] concerned finding the most suitable exchange-correlation energy functional of the GGA form to be applied for the systems of our interest. We chose relevant complexes formed by benzene, the basic constituent of PAHs, and diatomic molecules (N_2, O_2, and CO). Energetics and structural data concerning these complexes derived from various experiments are available in the literature,[25−31] and using these experimental data as reference data, we performed an exploratory study of possible computational approaches to study such systems. These studies showed that different approximate functionals for the exchange-correlation energy lead to qualitatively different results; LDA systematically overestimates the attraction energy, whereas the results obtained with GGA depend critically on the choice of the functional. For example, the B88P86 functional[32,33] overestimates the repulsion in such a way that the shallow minimum that was observed on the potential energy curve disappears when the curve is corrected for basis set superposition error (BSSE). The PW91 functional[34] was shown to lead to interaction energies in qualitative agreement with experiment and Møller−Plesset calculations. It is important to note that the mathematical form of the PW91 exchange-energy functional differs qualitatively from that of other commonly used GGA functionals. It cuts out smoothly the contributions to the exchange energy that arise from low electron densities. Moreover, its behavior ensures that the Lieb−Oxford bound,[35] an exact mathematical condition, is satisfied (see also other relevant papers dealing with the importance of this condition in the context of weak interactions[36,37]). The conclusion emerging from our work on benzene complexes[21] and that of Yang and co-workers[22] on rare-gas dimers was that the divergence of some of the enhancement factors applied in GGA leads to a repulsion artifact in the interaction energy. The PW91 and PBE[37] functionals are free from this artifact because they obey the Lieb−Oxford bound. This conclusion was confirmed by several subsequent papers of other authors following our suggestion.[38−40]

In a subsequent paper dealing with the same type of complexes,[41] we explored the applicability of another DFT route that is based on a partitioning of the electron density.[42,43] In this formalism, the total energy of a molecular complex A−B is expressed as a bifunctional, $E[\rho_A,\rho_B]$, of the electron densities of systems A and B (ρ_A and ρ_B), and the energy is minimized by varying independently ρ_A and ρ_B. As a result, each density ρ_A and ρ_B can be obtained from one-electron Kohn−Sham-like equations (Kohn−Sham equations with constrained electron Density, KSCED), the details of the numerical implementation of this approach being given in the methods section. Our previous work[41] concerning the C_6H_6−X complexes (X = N_2, O_2, and CO), recent studies of benzene dimer,[44] and complexes involving carbazole[45] showed that KSCED leads to very accurate interaction energies (the error being less than 20%). It is worthwhile to point out that the use of the total energy bifunctional to derive the interaction energy of weakly bound complexes is not new in quantum chemistry. It was already applied in 1972 by Gordon and Kim,[46] leading to astonishingly good interaction energies of rare-gas dimers. Opposite to the formalism applied in this work (KSCED), the model of Gordon and Kim is not variational.

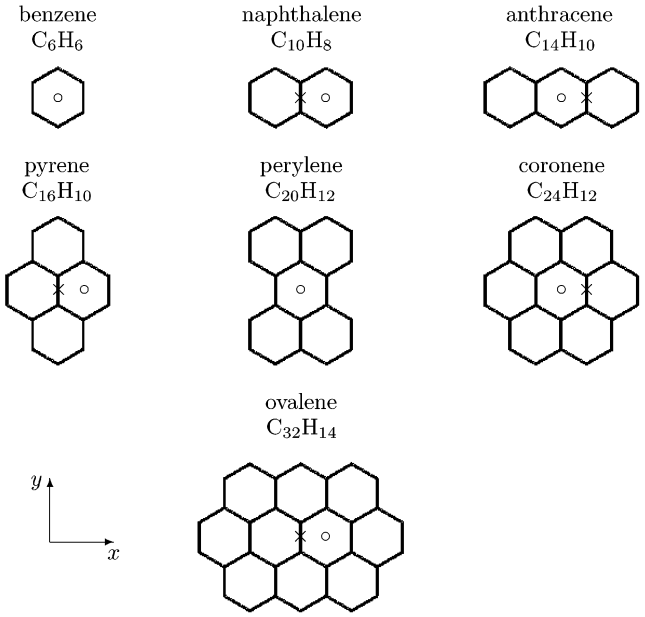

Figure 1. Polycyclic aromatic hydrocarbons (PAH) considered in this work. The *z* axis is perpendicular to the PAH plane.

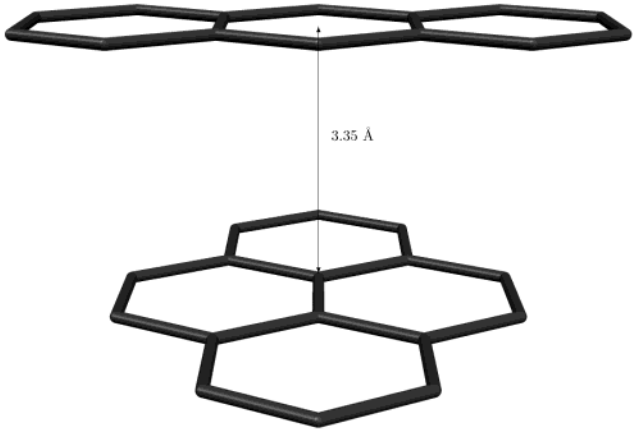

Figure 2. Two-layer compound formed by an anthracene molecule stacked on top of a pyrene molecule separated by a distance of 3.35 Å. The center of anthracene is located above the indicated carbon atom of pyrene.

In this work, we report the results of a systematic study of the complexes formed by molecular hydrogen with PAHs of increasing size (Figures 1 and 2), which can be considered as a series of cluster models of the extended (0001) surface of graphite. The equilibrium geometries and interaction energies were obtained by means of the subsystem-based approach (KSCED).

For comparison purposes, we applied also supermolecular calculations to derive these quantities for some of the considered complexes: Kohn−Sham with two different GGA functionals and Møller−Plesset (MP2).[47] Some calculations with the Kohn−

Sham approach on these systems, which employed the LDA, GGA, or hybrid functionals, have been reported in the literature (see refs 48 and 49 and Sidis et al. in ref 1).

Adsorption of molecular hydrogen on graphite surface was studied by means of various experimental techniques leading to the value of the interaction energy falling into the 1.1 and 1.2 kcal/mol range.[50] In particular, the values of $D_e = 1.19$ kcal/mol for the well depth and $z_m = 2.87$ Å for the surface-molecule distance were deduced from scattering experiments.[51] These values will be used in all comparisons throughout the paper.

II. Methods

We start with a short outline of the Kohn−Sham method, the most commonly used DFT formalism. This will provide a necessary reference to the subsystem-based approach applied in this work. According to Hohenberg−Kohn theorems,[17] the total ground-state energy of an electron system (atom, molecule, or solid, for instance) can be expressed as a functional of the electron density ($E = E[\rho]$). In the conventional Kohn−Sham formalism,[20] $E[\rho]$ is expressed using the Kohn−Sham (KS) total energy functional, $E^{KS}[\rho]$ (atomic units are used in all equations),

$$E^{KS}[\rho] = T_s[\rho] + J[\rho] + E_{xc}[\rho] - \sum_A \int \frac{Z_A}{|\mathbf{r} - \mathbf{R}_A|}\rho(\mathbf{r})\, d\mathbf{r} \quad (1)$$

where

$$J[\rho] = \frac{1}{2}\int\int \frac{\rho(\mathbf{r})\rho(\mathbf{r}')}{|\mathbf{r} - \mathbf{r}'|}\, d\mathbf{r}\, d\mathbf{r}' \quad (2)$$

$T_s[\rho]$ is the functional of the kinetic energy in the noninteracting electrons reference system, and $E_{xc}[\rho]$ is the exchange-correlation energy functional, which accounts for the quantum many-body effects. The exact analytical form of $E_{xc}[\rho]$ is unknown, and therefore, any practical calculations apply its approximations. The last term of eq 1 represents the electron−nucleus attraction energy, where index A runs over all nuclei of charge Z_A positioned at $\mathbf{R}_A$. The variational principle leads to the one-electron self-consistent Kohn−Sham equations

$$\left(-\frac{1}{2}\nabla^2 + \nu_{eff}(\mathbf{r})\right)\psi_i(\mathbf{r}) = \epsilon_i\psi_i(\mathbf{r}) \quad (3)$$

where

$$\nu_{eff}(\mathbf{r}) = \int \frac{\rho(\mathbf{r}')}{|\mathbf{r} - \mathbf{r}'|}\, d\mathbf{r}' + \frac{\delta E_{xc}[\rho]}{\delta\rho(\mathbf{r})} - \sum_A \frac{Z_A}{|\mathbf{r} - \mathbf{R}_A|} \quad (4)$$

and

$$\rho(\mathbf{r}) = \sum_{i=1}^{N} |\psi_i(\mathbf{r})|^2 \quad (5)$$

Using the Kohn−Sham orbitals derived from eqs 3−5, one can calculate the functional $T_s[\rho]$:

$$T_s[\rho] = -\frac{1}{2}\sum_{i=1}^{N} \int \psi_i^*(\mathbf{r})\nabla^2\psi_i(\mathbf{r})\, d\mathbf{r} \quad (6)$$

and hence the total energy, $E[\rho]$.

The Kohn−Sham calculations were performed with the PW91 functional for the exchange-correlation energy,[34] and as it has already been said, this functional seems to be one of the best for weakly bound systems. PW91 is also the functional that was chosen for the KSCED calculations (see below). Calculations for the benzene−H_2 complex were also made with the mPW functional of Adamo and Barone[36] (its exchange part is a reparametrization of the PW91 one and its correlation part is exactly the same as the PW91 one). Several basis sets of increasing flexibility (see Table 1) were employed for the complex benzene−H_2: the standard 6-311++G**, two correlation-consistent basis sets proposed by Dunning and coworkers, aug-cc-pVTZ and aug-cc-pVQZ,[52] and an uncontracted basis set developed by Partridge.[53] Unless specified, the potential energy surface was corrected for BSSE by means of the counterpoise technique of Boys and Bernardi.[54] The Kohn−Sham calculations were performed with the Gaussian package.[55]

TABLE 1: The Basis Sets Used in This Work and Their Contraction

basis set	element	contraction
6-311++G**	H	(6s,1p) → [4s,1p]
6-311++G**	C	(12s,6p,1d) → [5s,4p,1d]
aug-cc-pVTZ	H	(6s,3p,2d) → [4s,3p,2d]
aug-cc-pVTZ	C	(11s,6p,3d,2f) → [5s,4p,3d,2f]
aug-cc-pVQZ	H	(7s,4p,3d,2f) → [5s,4p,3d,2f]
aug-cc-pVQZ	C	(13s,7p,4d,3f,2g) → [6s,5p,4d,3f,2g]
TZVP	H	(5s,2p) → [2s,2p]
TZVP	C	(10s,6p,1d) → [4s,3p,1d]
Partridge	H	(7s,4p) → [7s,4p]
Partridge	C	(13s,8p,4d) → [13s,8p,4d]

The subsystem-based formalism applied in this work was described in detail elsewhere.[56] Here, only its outline and the details of its implementation specific to this work are presented. The total energy of a system composed of two subsystems (two molecules forming a van der Waals complex, for instance) of densities ρ_1 and ρ_2 is represented as the bifunctional $E[\rho_1,\rho_2] = E^{KSCED}[\rho_1,\rho_2]$ of ρ_1 and ρ_2[46]

$$E^{KSCED}[\rho_1,\rho_2] = T_s[\rho_1] + T_s[\rho_2] + T_s^{nadd}[\rho_1,\rho_2] + \frac{1}{2}\int\int \frac{(\rho_1(\mathbf{r}) + \rho_2(\mathbf{r}))(\rho_1(\mathbf{r}') + \rho_2(\mathbf{r}'))}{|\mathbf{r} - \mathbf{r}'|}\, d\mathbf{r}\, d\mathbf{r}' + E_{xc}[\rho_1 + \rho_2] - \sum_A \int \frac{Z_A}{|\mathbf{r} - \mathbf{R}_A|}(\rho_1(\mathbf{r}) + \rho_2(\mathbf{r}))\, d\mathbf{r} \quad (7)$$

where $T_s^{nadd}[\rho_1,\rho_2]$ denotes the nonadditive kinetic-energy bifunctional, which is defined as

$$T_s^{nadd}[\rho_1,\rho_2] = T_s[\rho_1 + \rho_2] - T_s[\rho_1] - T_s[\rho_2] \quad (8)$$

As in the case of the exchange-correlation energy functional, the exact orbital-free analytical form of $T_s^{nadd}[\rho_1,\rho_2]$ is unknown and any practical calculations rely on approximations. Partitioning the electron density makes it possible to perform a constrained minimization of $E[\rho_1,\rho_2]$ in which one of the components (ρ_1 for instance) is allowed to vary whereas the other (ρ_2) is frozen.[43]

In practice, the electron density (ρ_J, $J = 1$ or 2) that minimizes the total energy bifunctional can be obtained from a numerical procedure closely resembling that applied in the Kohn−Sham method. For subsystem J comprising N_J electrons, ρ_J is represented by means of one-electron orbitals, $\psi_{i(J)}$:

$$\rho_J(\mathbf{r}) = \sum_{i=1}^{N_J} |\psi_{i(J)}(\mathbf{r})|^2 \quad (9)$$

Similar steps as those used to derive Kohn−Sham equations lead to the following one-electron Kohn−Sham-like equations for $\psi_{i(J)}$:[42,43]

$$\left(-\frac{1}{2}\nabla^2 + v_{\mathrm{eff}(J)}^{\mathrm{KSCED}}(\mathbf{r})\right)\psi_{i(J)}(\mathbf{r}) = \epsilon_{i(J)}\psi_{i(J)}(\mathbf{r}) \qquad (10)$$

where

$$v_{\mathrm{eff}(J)}^{\mathrm{KSCED}}(\mathbf{r}) = \frac{\delta T_{\mathrm{s}}^{\mathrm{nadd}}[\rho_1,\rho_2]}{\delta\rho_J(\mathbf{r})} + \int\frac{\rho_1(\mathbf{r}')}{|\mathbf{r}-\mathbf{r}'|}\,\mathrm{d}\mathbf{r}' + \int\frac{\rho_2(\mathbf{r}')}{|\mathbf{r}-\mathbf{r}'|}\,\mathrm{d}\mathbf{r}' + \frac{\delta E_{\mathrm{xc}}[\rho_1+\rho_2]}{\delta\rho_J(\mathbf{r})} - \sum_A\frac{Z_A}{|\mathbf{r}-\mathbf{R}_A|} \qquad (11)$$

The above one-electron equations were used by Wesołowski and Warshel to introduce the first-principles-based orbital-free embedding effective potential to study solvated molecules.[43] It is, however, general; it uses universal (system-independent) functionals defined in density functional theory and expresses the $T_{\mathrm{s}}^{\mathrm{nadd}}[\rho_1,\rho_2]$ bifunctional, which is of purely quantum mechanical origin, in an orbital-free way. In the case of such problems in which only the properties of one of the two subsystems are of primary interest, KSCED provides a computationally efficient and system-independent theoretical framework. For the most recent applications of the KSCED embedding effective potential, see ref 57 and references therein.

In this work, we apply KSCED in such a way that both ρ_1 and ρ_2 are equally important. In such a case, ρ_1 and ρ_2, which minimize the total energy bifunctional $E[\rho_1,\rho_2]$, can be obtained by means of a stepwise procedure ("freeze-and-thaw") in which ρ_1 and ρ_2 are varied in a series of successive minimizations.[58] The KSCED calculations were performed using the modified version of the deMon program into which the KSCED formalism was implemented.[59] The two subsystems corresponding to electron densities ρ_1 and ρ_2 were identified with the PAH and H_2 molecules. On the basis of our previous studies, the PW91 functional was chosen for the exchange-correlation energy, and the terms $T_{\mathrm{s}}[\rho]$ in the nonadditive kinetic energy $T_{\mathrm{s}}^{\mathrm{nadd}}[\rho_1,\rho_2]$ were approximated using the GGA functional constructed following the conjointness conjecture of Lee, Lee, and Parr.[60] The analytical form of the gradient-dependency of $T_{\mathrm{s}}^{\mathrm{nadd}}[\rho_1,\rho_2]$ is the same as that of the applied exchange-energy functional, that is, that of the PW91 functional.[56,61]

The basis sets used in the KSCED calculations were chosen on the basis of our previous works dealing with the dependence of the KSCED results on the expansion of the electron density of each subsystem by means of orbitals localized on atoms.[44,45] The calculations were carried out using two different orbital basis sets (see Table 1): the first basis is triple-ζ valence with polarization (TZVP),[62] and the second one is the Partridge[53] basis set. The electron density of each subsystem (ρ_J, $J = 1$ or 2) was expanded using only the atomic orbitals localized on the same subsystem (J). This is an appropriate approximation for interacting subsystems in which such effects as charge transfer between subsystems or orbital interactions are negligible (for more details, see ref 56). If such localized expansion of the electron densities is applied, the quality of the basis set does not change with geometry, resulting in the KSCED interaction energies being BSSE-free.

III. Results and Discussion

Adsorption of molecular hydrogen on eight different molecules was investigated. Seven of them are planar PAHs ranging from benzene, C_6H_6, to ovalene, $C_{32}H_{14}$ (Figure 1), and can be seen as a series of models of the infinite (0001) graphite surface. The two-layer compound in Figure 2 formed by an anthracene molecule stacked on top of a pyrene unit at the distance of 3.35 Å (equal to the distance between two planes in solid graphite) is a model molecular association designed to mimic the accretion of the carbonaceous dust. In geometry optimization, only the intermolecular degrees of freedom were varied. For each PAH, R_{CC} was kept at 1.42 Å, corresponding to the CC distance in graphite, and R_{CH} was kept at 1.10 Å. For H_2, R_{HH} was kept at 0.74 Å as in the isolated molecule.

TABLE 2: Interaction Energy (ΔE) for the $C_6H_6-H_2$ Complex Obtained by Means of Various Methods, Kohn−Sham (KS) with PW91 or mPW Exchange-Correlation Energy Functional, KSCED, and MP2[a]

method	basis set	orientation of H_2	z_{m} (Å)	ΔE (kcal/mol)
KS/PW91	6-311++G**	*X*	3.35	−0.42
	aug-cc-pVTZ	*X*	3.45	−0.43
	aug-cc-pVQZ	*X*	3.46	−0.43
	Partridge	*X*	3.45	−0.41
KS/mPW	6-311++G**	*X*	*b*	*b*
	Partridge	*X*	*b*	*b*
KSCED	TZVP	*X*	2.66	−1.16
	Partridge	*X*	2.70	−1.17
	TZVP	*Y*	2.64	−1.17
	Partridge	*Y*	2.66	−1.19
	TZVP	*Z*	2.88	−1.18
	Partridge	*Z*	2.89	−1.26
MP2	6-311++G**	*X*	3.27	−0.30
	aug-cc-pVTZ	*X*	3.01	−0.80
	aug-cc-pVQZ	*X*	3.01[c]	−0.86
	6-311++G**	*Z*	3.30	−0.64
	aug-cc-pVTZ	*Z*	3.09	−1.14
	aug-cc-pVQZ	*Z*	3.09[c]	−1.21

[a] *X*, *Y*, or *Z* indicates the orientation of the H_2 axis (see Figure 1). The position of the center of mass of H_2 is above the center of the benzene ring, and z_{m} denotes its vertical distance from the benzene plane. The results derived from supermolecular calculations (KS and MP2) are corrected for BSSE. [b] No minimum. [c] Single point at the aug-cc-pVTZ minimum.

For different orientations of H_2, the minimum energy distance (z_{m}) between the surface and the center of mass of the H_2 molecule was found by means of single-point energy calculations. Three orientations of H_2 were considered, *X*, *Y*, and *Z*, which correspond to the axis of the H_2 molecule being oriented parallel to the directions *x*, *y*, and *z* (defined in Figure 1), respectively. The center of mass of H_2 was localized above the center of a ring in most of the calculations as indicated with ○ in Figure 1. Additional calculations were also made in which the center of mass of H_2 was localized above the center of a CC bond as indicated with × in Figure 1.

We start the discussion of our results with the supermolecular MP2 calculations made for the two smallest considered complexes, benzene−H_2 and naphthalene−H_2. The calculations were performed with the Gaussian package.[55] For the smaller of these complexes, three basis sets were used (6-311++G**, aug-cc-pVTZ, and aug-cc-pVQZ). For the larger complex, only the 6-311++G** basis set was used. The results of these MP2 calculations, which provide additional reference data, are collected in Tables 2 and 3. The MP2 results for the benzene−H_2 complex clearly show that the use of the correlation-consistent basis set aug-cc-pVTZ is indispensable because it affects the interaction energy by as much as 0.5 kcal/mol compared to the 6-311++G** one. For the naphthalene−H_2

TABLE 3: BSSE-Corrected Interaction Energy (ΔE) of $C_{10}H_8-H_2$ Obtained from MP2 Calculations with 6-311++G Basis Set[a]**

orientation of H_2	position of H_2	z_m (Å)	ΔE (kcal/mol)
X	○	3.18	−0.61
Z	○	3.25	−0.85
X	×	3.26	−0.47
Z	×	3.32	−0.64

[a] *X* or *Z* indicates the orientation of the H_2 axis (see Figure 1). The symbol ○ or × indicates that the position of the center of mass of H_2 is located above either a ring center or a CC bond of $C_{10}H_8$, whereas z_m denotes its vertical distance from the $C_{10}H_8$ plane.

TABLE 4: Interaction Energies (ΔE) for the Considered PAH$-H_2$ Complexes Obtained from Supermolecular BSSE-Corrected Kohn−Sham Calculations (PW91 Exchange-Correlation Energy Functional and 6-311++G Basis Set)[a]**

cluster	orientation of H_2	position of H_2	z_m (Å)	ΔE (kcal/mol)
$C_6H_6-H_2$	*X*	○	3.35	−0.42
	Y	○	3.35	−0.42
	Z	○	3.32	−0.75
$C_{14}H_{10}-H_2$	*X*	○	3.42	−0.47
	Y	○	3.34	−0.43
	Z	○	3.41	−0.57
$C_{20}H_{12}-H_2$	*X*	○	3.44	−0.44
	Y	○	3.42	−0.48
	Z	○	3.54	−0.47
$C_{24}H_{12}-H_2$	*X*	○	3.44	−0.45
	Y	○	3.44	−0.45
	Z	○	3.50	−0.47
$C_{32}H_{14}-H_2$	*X*	○	3.41	−0.46
	Y	○	3.41	−0.46
	Z	○	3.46	−0.48
$C_{16}H_{10}-C_{14}H_{10}-H_2$	*X*	○	3.48	−0.46
	Y	○	3.40	−0.42
	Z	○	3.45	−0.57

[a] *X*, *Y*, or *Z* indicates the orientation of the H_2 axis (see Figure 1). ○ indicates that the position of the center of mass of H_2 is above the center of a PAH ring, whereas z_m denotes its vertical distance from the PAH plane.

complex (Table 3), the largest interaction energy derived from MP2/6-311++G** calculations equals −0.85 kcal/mol for the *Z* orientation above the ring center. Assuming that increase of the basis set results in a similar effect on the interaction energy for this complex as it was seen for the smaller one, we can estimate an MP2 well depth of about 1.5 kcal/mol, a value which is consistent with experimental estimates (1.1−1.2 kcal/mol).[50,51]

A. Kohn−Sham Calculations. *1. Benzene−H_2 Complex.* For the smallest considered complex, we applied various methods to perform supermolecular calculations: Kohn−Sham with the PW91 exchange-correlation functional (also applied in KSCED calculations), Kohn−Sham with the mPW exchange-correlation functional, and MP2 (already discussed above). As shown in Table 2, PW91 leads to an interaction energy of about −0.4 kcal/mol for the *X* orientation with all of the basis sets and a distance of $z_m = 3.35$ Å with 6-311++G**, which is shorter by about 0.1 Å compared to the values obtained with the larger basis sets. The mPW functional does not lead to any minimum for the *X* orientation, either with 6-311++G** or with the Partridge basis set.

Table 4 collects the results obtained for the three orientations *X*, *Y*, and *Z* of the H_2 molecule with the PW91 functional and 6-311++G** basis set. Among the three orientations, the one with the greatest interaction energy ($\Delta E = -0.75$ kcal/mol) is that in which H_2 is perpendicular to the benzene plane with $z_m = 3.32$ Å. The *X* and *Y* orientations, in which H_2 is parallel to the benzene plane, correspond to less-stable structures ($\Delta E = -0.42$ kcal/mol). Compared to the MP2/aug-cc-pVQZ results of Table 2, the PW91 interaction energies are underestimated by about 0.45 kcal/mol and the values for z_m are overestimated by about 0.3 Å.

2. From Anthracene−H_2 to Ovalene−H_2 Complexes. Table 4 shows that the perpendicular orientation (*Z*) remains the most stable also in the complexes comprising larger PAHs. The energetic preference for the *Z* orientation over the parallel ones, found for the benzene−H_2 complex, becomes significantly reduced upon increasing the number of aromatic rings surrounding the adsorption site (from 0.3 kcal/mol for benzene through 0.1 kcal/mol for anthracene, which comprises two adjacent rings, down to 0.02 kcal/mol for coronene, which comprises six adjacent rings). For the largest cluster model of graphite (ovalene), this energetic preference is barely significant. The complex involving perylene is slightly different because the dominant electronic structure of this compound is more similar to that of two naphthalene units connected by two CC bonds than that of an evenly delocalized PAH. Even in this particular case, the difference between the parallel and perpendicular orientations amounts to only 0.01 kcal/mol favoring the parallel *Y* orientation. Concerning the geometries of the complexes, the distance z_m between the center of mass of H_2 and the surface increases from about 3.35 Å for the benzene complex to about 3.45 ± 0.05 Å for the complexes involving larger PAHs, which is about 0.6 Å larger than the experimental value of 2.87 Å.

3. Two-Layer Pyrene−Anthracene−H_2 Complex. The sandwich complex of pyrene−anthracene provides a two-layer model of the graphite surface. Comparison with the previously described results obtained for anthracene−H_2 complex makes it possible to estimate the effects of the second layer. The structure calculated for this complex is similar to that found for anthracene−H_2. The second layer, represented by a pyrene unit, does not affect significantly the structure because the distance from the surface is lengthened by only 0.05 Å. This geometrical effect is similar for all of the considered orientations of H_2.

4. Importance of the Basis Set Superposition Error. All of the Kohn−Sham and MP2 equilibrium geometries and interaction energies reported so far were obtained using potential energy surfaces corrected for BSSE. The fact that the BSSE artifact depends on the geometry of the complex requires the BSSE correction to be made for each point on the potential energy surface, which means that the correcting scheme, the counterpoise procedure,[54] has to be incorporated in the minimization procedure itself. Not correcting this spurious behavior, or even correcting the results after the optimized structure has been obtained, may result in erroneous results, especially for weakly bound systems.[38,63,64] The values of z_m derived from Kohn−Sham calculations are systematically shorter than their BSSE-corrected counterparts. For the complexes involving large PAHs, that is, those with 5−10 benzene rings, the typical BSSE effects on equilibrium distances is about 0.13−0.15 Å. Similarly, BSSE leads to a typical stabilization artifact of about 0.15−0.20 kcal/mol for the corresponding structures.

The main conclusions from the above Kohn−Sham calculations can be summarized as follows: (1) In the series of cluster models of graphite surface of increasing size, the interaction energy stabilizes around −0.45 kcal/mol. (2) For the largest

TABLE 5: Interaction Energies (ΔE) for the Considered PAH−H_2 Complexes Obtained by Means of the Subsystem-Based Approach KSCED and Using the TZVP Basis Set (see Table 1)[a]

cluster	orientation of H_2	position of H_2	z_m (Å)	ΔE (kcal/mol)
$C_6H_6-H_2$	*X*	○	2.66	−1.16
	Y	○	2.64	−1.17
	Z	○	2.88	−1.18
$C_{10}H_8-H_2$	*X*	○	2.66	−1.19
	Y	○	2.62	−1.20
	Z	○	2.89	−1.09
	X	×	2.77	−1.13
	Y	×	2.78	−1.05
	Z	×	2.99	−0.98
$C_{14}H_{10}-H_2$	*X*	○	2.66	−1.22
	Y	○	2.61	−1.23
	Z	○	2.89	−1.00
	X	×	2.78	−1.11
	Y	×	2.77	−1.06
	Z	×	2.99	−0.96
$C_{16}H_{10}-H_2$	*X*	○	2.64	−1.23
	Y	○	2.63	−1.23
	Z	○	2.89	−1.00
	X	×	2.80	−1.08
	Y	×	2.79	−1.10
	Z	×	2.99	−0.93
$C_{20}H_{12}-H_2$	*X*	○	2.64	−1.26
	Y	○	2.61	−1.31
	Z	○	2.90	−0.90
$C_{24}H_{12}-H_2$	*X*	○	2.65	−1.25
	Y	○	2.62	−1.26
	Z	○	2.89	−0.92
	X	×	2.80	−1.08
	Y	×	2.79	−1.10
	Z	×	2.99	−0.91
$C_{32}H_{14}-H_2$	*X*	○	2.65	−1.24
	Y	○	2.62	−1.27
	Z	○	2.89	−0.92
	X	×	2.80	−1.08
	Y	×	2.79	−1.10
	Z	×	2.98	−0.90
$C_{16}H_{10}-C_{14}H_{10}-H_2$	*X*	○	2.66	−1.21
	Y	○	2.62	−1.22
	Z	○	2.89	−1.03

[a] *X*, *Y*, or *Z* indicates the orientation of the H_2 axis (see Figure 1). The symbol ○ or × indicates that the position of the center of mass of H_2 is located above either a ring center or a CC bond of the PAH, whereas z_m denotes its vertical distance from the PAH plane.

clusters, all of the orientations of the adsorbed H_2 molecule are energetically equivalent. (3) The presence of the second layer in the cluster model of the graphite surface does not affect the calculated interaction energies.

B. KSCED Calculations. *1. Benzene−H_2 Complex.* The results obtained with the TZVP basis set (see Table 5) show that the three orientations (*X*, *Y*, and *Z*) of H_2, localized above the center of the ring, are energetically equivalent ($-1.18 \leq \Delta E \leq -1.16$ kcal/mol). The differences between the calculated ΔE at various orientations are on the order of 0.01 kcal/mol. For the *Z* orientation, the center of mass of H_2 is located at about 2.9 Å above the benzene plane, which is higher than that for the *X* and *Y* orientations (∼2.65 Å). As the choice of the basis set is concerned, the calculations were repeated using a larger one (Partridge basis set). This change affects little the results (Table 2); the maximum change in the interaction energy amounting to 0.08 kcal/mol occurs for the *Z* orientation ($\Delta E = -1.26$ kcal/mol). For the *X* and *Y* orientations, the change is smaller (0.01−0.02 kcal/mol). Similarly, the effect of the change of the basis set on the position of the energy minima is not significant. Equilibrium distances for the *X* and *Y* orientations are lengthened by at most 0.04 Å. These results agree with the trends found for other weakly bound complexes studied using the KSCED formalism.[41,44,45] The small energetic effect accompanying the change of the basis set led us to the choice of TZVP to be used in the KSCED calculations for larger clusters. As the comparisons between MP2 and KSCED calculations are concerned, they are in a good agreement. For the *Z* orientation, the KSCED and MP2/aug-cc-pVQZ interaction energies differ by less than 0.05 kcal/mol, and for the *X* orientation, the KSCED method gives an interaction energy that is stronger by about 0.3 kcal/mol. The KSCED values for z_m are smaller than the ones obtained with MP2/aug-cc-pVTZ (by about 0.3 Å for the *X* orientation and 0.2 Å for the *Z* orientation).

2. From Naphthalene−H_2 to Ovalene−H_2 Complexes. For larger clusters in the series of cluster models of increasing size, the interaction energy stabilizes at about −1.25 kcal/mol for the parallel *X* and *Y* orientations. For ovalene, which is the largest PAH considered in this work, the most stable geometry corresponds to *Y*-oriented H_2 located at 2.62 Å above the center of a ring (○ in Figure 1) ($\Delta E = -1.27$ kcal/mol). The calculated interaction energy of the perpendicular *Z* orientation stabilizes at −0.92 kcal/mol. Moving the center of mass of H_2 from above the ring center to above the center of one of the central CC bonds (× in Figure 1) decreases the interaction energy of the parallel orientations of the largest PAH−H_2 complexes by about 0.15 kcal/mol. This trend is in line with previous reports on the adsorption of molecular hydrogen on coronene.[48,49] Moving the H_2 molecule to a position above one of the carbon atom tends to decrease further the magnitude of the interaction energies.

3. Two-Layer Pyrene−Anthracene−H_2 Complex. As in the case of the Kohn−Sham calculations, the addition of a second layer does not affect significantly the values obtained for the interaction energies and equilibrium distances. Comparing the results obtained for the anthracene−H_2 complex with that for the pyrene−anthracene−H_2 complex, collected in Table 5, shows that the pyrene−anthracene interactions do not affect significantly either the interaction energies (affected by less than 0.03 kcal/mol) or the minimum energy structures (affected by less than 0.01 Å).

IV. Conclusion

This study clearly shows that molecular hydrogen can be easily depleted on PAHs or graphite dust particles in low-temperature conditions. The interaction energy does not depend strongly on the number of aromatic rings of the PAH molecule or on the number of layers used to represent the graphite surface. This indicates that the values obtained with the largest clusters (coronene and ovalene) can be used as a good estimate of the adsorption energy of molecular hydrogen on infinite graphite surface and that essentially the same sticking probability can be expected for macroscopic graphite-like surfaces as for various PAHs, free flyers in the interstellar space. Our best estimate of the interaction energy of about 1.25 kcal/mol corresponds to a temperature of about 600 K, largely above that of most of interstellar clouds. Therefore, one can expect that a significant fraction of molecular hydrogen present in interstellar space can be trapped on carbonaceous surfaces and escapes detection.

As the DFT methodologies are concerned, this study shows that the KSCED interaction energies obtained for the smallest clusters (benzene−H_2 and naphthalene−H_2) are in a good agreement with the MP2 values. Moreover, the KSCED results

obtained for the largest cluster model (ovalene−H_2) can be used for comparisons with the experimental results concerning adsorption of molecular hydrogen on graphite. These comparisons indicate that the KSCED calculations lead to a very good agreement with experimental measurements. The good performance of the KSCED(GGA) method as compared to the supermolecular KS(GGA) one results from the different relative contribution of the approximate terms in these two approaches. In Kohn−Sham calculations, the GGA results for weakly bound complexes are critically dependent on the choice of the gradient-dependency of the applied exchange-correlation functional.[21] In KSCED(GGA) calculations, approximate functionals are used for the exchange-correlation part of the total energy as well as for the nonadditive kinetic energy part, and as a result, the choice of the analytic form of the gradient-dependency affects less the final interaction energies. This partial cancellation of approximate terms was pointed out in our earlier works[41,65] and was discussed in detail in our recent paper.[45]

The KSCED minimum-energy geometry corresponds to a parallel orientation of H_2 to the graphite surface located at a distance of 2.62 Å above the surface, which is in fair agreement with the equilibrium distance of $z_m^{exp} = 2.87$ Å derived from scattering experiments of H_2 on graphite surface. It is worthwhile to underline, however, that for the perpendicular orientation of H_2 our KSCED calculations lead to the equilibrium distance of 2.89 Å with the interaction energy of −0.92 kcal/mol. The supermolecular GGA (PW91) Kohn−Sham results presented in this study show the same trends, rapid convergence of the interaction energy with the size of the cluster and negligible effect of the second graphite layer on the energetics and position of physisorbed molecular hydrogen. The interaction energy is, however, significantly underestimated in agreement with results available in the literature for other complexes involving aromatic rings.[21,39]

Acknowledgment. Financial support by the Federal Office for Education and Science, acting as Swiss COST office, is greatly acknowledged. This work is also part of the Project 21-63645.00 of the Swiss National Science Foundation. T.A.W. acknowledges the computer equipment grants from *Fonds Frédéric Firmenich et Philippe Chuit* and *Fondation Ernst et Lucie Schmidheiny*. This research was also supported by CNRS "Programme National de Physique et Chimie du Milieu Interstellaire". Part of the calculations presented in this contribution were financed by the CNRS-IDRIS supercomputing center.

References and Notes

(1) *Molecular Hydrogen in Space*; Combes, F., Pineau des Forêts, G., Eds.; Cambridge University Press: Cambridge,U.K., 2000.
(2) Barlow, M. J.; Silk, J. *Astrophys. J.* **1976**, *207*, 131.
(3) Parneix, P.; Bréchignac, Ph. *Astron. Astrophys.* **1998**, *334*, 363.
(4) Kim, Y. H.; Ree, J.; Shin, H. K. *Chem. Phys. Lett.* **1999**, *314*, 1.
(5) Ree, J.; Kim, Y. H.; Shin, H. K. *Chem. Phys. Lett.* **2002**, *353*, 368.
(6) Farebrother, A. J.; Meijer, A. J. H. M.; Clary, D. C.; Fisher, A. J. *Chem. Phys. Lett.* **2000**, *319*, 303.
(7) Meijer, A. J. H. M.; Farebrother, A. J.; Clary, D. C.; Fisher, A. J. *J. Phys. Chem. A* **2001**, *105*, 2173.
(8) Jackson, B.; Lemoine, D. *J. Chem. Phys.* **2001**, *114*, 474.
(9) Sha, X.; Jackson, B. *Surf. Sci.* **2002**, *496*, 318.
(10) Sha, X.; Jackson, B.; Lemoine, D. *J. Chem. Phys.* **2002**, *116*, 7158.
(11) Rutigliano, M.; Cacciatore, M.; Billing, G. D. *Chem. Phys. Lett.* **2001**, *340*, 13.
(12) Marty, P.; Serra, G.; Chaudret, B.; Ristorcelli, I. *Astron. Astrophys.* **1994**, *282*, 916.
(13) Allamandola, L. J. *Top. Curr. Chem.* **1990**, *153*, 1.
(14) Salama, F. In *Solid Interstellar Matter: ISO Revolution, Les Houches Workshop*; D'Hendecourt, L., Joblin, C., Jones, A., Eds.; Springer: Berlin, 1999; p 65.
(15) Leger, A.; Puget, J. L. *Astron. Astrophys.* **1984**, *137*, L5.
(16) Allamandola, L. J.; Tielens, A. G. G. M.; Barker, J. R. *Astrophys. J. Lett.* **1985**, *290*, L25.
(17) Hohenberg, P.; Kohn, W. *Phys. Rev.* **1964**, *136*, B864.
(18) Parr, R. G.; Yang, W. *Density-Functional Theory of Atoms and Molecules*; Oxford University Press: New York, 1989.
(19) Wesołowski, T. A. *J. Chem. Phys.* **2000**, *113*, 1666.
(20) Kohn, W.; Sham, L. J. *Phys. Rev.* **1965**, *140*, A1133.
(21) Wesołowski, T. A.; Parisel, O.; Ellinger, Y.; Weber, J. *J. Phys. Chem. A* **1997**, *101*, 7818.
(22) Zhang, Y.; Pan, W.; Yang, W. *J. Chem. Phys.* **1997**, *107*, 7921.
(23) Kristyán, S.; Pulay, P. *Chem. Phys. Lett.* **1994**, *229*, 175.
(24) Pérez-Jordá, J. M.; Becke, A. D. *Chem. Phys. Lett.* **1995**, *233*, 134.
(25) Gooding, E. A.; Serak, K. R.; Ogilby, P. R. *J. Phys. Chem.* **1991**, *95*, 7868.
(26) Grover, J. R.; Hagenow, G.; Walters, E. A. *J. Chem. Phys.* **1992**, *97*, 628.
(27) Nowak, R.; Menapace, J. A.; Bernstein, E. R. *J. Chem. Phys.* **1988**, *89*, 1309.
(28) Weber, Th.; Smith, A. M.; Riedle, E.; Neusser, H. J.; Schlag, E. W. *Chem. Phys. Lett.* **1990**, *175*, 79.
(29) Ernstberger, B.; Krause, H.; Neusser, H. J. *Z. Phys. D* **1991**, *20*, 189.
(30) Ohshima, Y.; Kohguchi, H.; Endo, Y. *Chem. Phys. Lett.* **1991**, *184*, 21.
(31) Brupbacher, Th.; Bauder, A. *J. Chem. Phys.* **1993**, *99*, 9394.
(32) Becke, A. D. *Phys. Rev. A* **1988**, *38*, 3098.
(33) Perdew, J. P. *Phys. Rev. B* **1986**, *33*, 8822.
(34) Perdew, J. P.; Chevary, J. A.; Vosko, S. H.; Jackson, K. A.; Pederson, M. R.; Singh, D. J.; Fiolhais, C. *Phys. Rev. B* **1992**, *46*, 6671.
(35) Lieb, E. H.; Oxford, S. *Int. J. Quantum Chem.* **1981**, *19*, 427.
(36) Adamo, C.; Barone, V. *J. Chem. Phys.* **1998**, *108*, 664.
(37) Perdew, J. P.; Burke, K.; Ernzerhof, M. *Phys. Rev. Lett.* **1996**, *77*, 3865; **1997**, *78*, 1396(E). Zhang, Y.; Yang, W. *Phys. Rev. Lett.* **1998**, *80*, 890. Perdew, J. P.; Burke, K.; Ernzerhof, M. *Phys. Rev. Lett.* **1998**, *80*, 891.
(38) Couronne, O.; Ellinger, Y. *Chem. Phys. Lett.* **1999**, *306*, 71.
(39) Tsuzuki, S.; Lüthi, H. P. *J. Chem. Phys.* **2001**, *114*, 3949.
(40) Wu, X.; Vargas, M. C.; Nayak, S.; Lotrich, V.; Scoles, G. *J. Chem. Phys.* **2001**, *115*, 8748.
(41) Wesołowski, T. A.; Ellinger, Y.; Weber, J. *J. Chem. Phys.* **1998**, *108*, 6078.
(42) Cortona, P. *Phys. Rev. B* **1991**, *44*, 8454.
(43) Wesołowski, T. A.; Warshel, A. *J. Phys. Chem.* **1993**, *97*, 8050.
(44) Tran, F.; Weber, J.; Wesołowski, T. A. *Helv. Chim. Acta* **2001**, *84*, 1489.
(45) Wesołowski, T. A.; Morgantini, P.-Y.; Weber, J. *J. Chem. Phys.* **2002**, *116*, 6411.
(46) Gordon, R. G.; Kim, Y. S. *J. Chem. Phys.* **1972**, *56*, 3122.
(47) Møller, C.; Plesset, M. S. *Phys. Rev.* **1934**, *46*, 618.
(48) Arellano, J. S.; Molina, L. M.; Rubio, A.; Alonso, J. A. *J. Chem. Phys.* **2000**, *112*, 8114.
(49) Okamoto, Y.; Miyamoto, Y. *J. Phys. Chem. B* **2001**, *105*, 3470.
(50) Vidali, G.; Ihm, G.; Kim, H.-Y.; Cole, M. W. *Surf. Sci. Rep.* **1991**, *12*, 133.
(51) Mattera, L.; Rosatelli, F.; Salvo, C.; Tommasini, F.; Valbusa, U.; Vidali, G. *Surf. Sci.* **1980**, *93*, 515.
(52) Dunning, T. H., Jr. *J. Chem. Phys.* **1989**, *90*, 1007. Kendall, R. A.; Dunning, T. H., Jr.; Harrison, R. J. *J. Chem. Phys.* **1992**, *96*, 6796.
(53) Partridge, H. *J. Chem. Phys.* **1989**, *90*, 1043.
(54) Boys, S. F.; Bernardi, F. *Mol. Phys.* **1970**, *19*, 553.
(55) Frisch, M. J.; Trucks, G. W.; Schlegel, H. B.; Scuseria, G. E.; Robb, M. A.; Cheeseman, J. R.; Zakrzewski, V. G.; Montgomery, J. A., Jr.; Stratmann, R. E.; Burant, J. C.; Dapprich, S.; Millam, J. M.; Daniels, A. D.; Kudin, K. N.; Strain, M. C.; Farkas, O.; Tomasi, J.; Barone, V.; Cossi, M.; Cammi, R.; Mennucci, B.; Pomelli, C.; Adamo, C.; Clifford, S.; Ochterski, J.; Petersson, G. A.; Ayala, P. Y.; Cui, Q.; Morokuma, K.; Malick, D. K.; Rabuck, A. D.; Raghavachari, K.; Foresman, J. B.; Cioslowski, J.; Ortiz, J. V.; Stefanov, B. B.; Liu, G.; Liashenko, A.; Piskorz, P.; Komaromi, I.; Gomperts, R.; Martin, R. L.; Fox, D. J.; Keith, T.; Al-Laham, M. A.; Peng, C. Y.; Nanayakkara, A.; Gonzalez, C.; Challacombe, M.; Gill, P. M. W.; Johnson, B. G.; Chen, W.; Wong, M. W.; Andres, J. L.; Head-Gordon, M.; Replogle, E. S.; Pople, J. A. *Gaussian 98*, revision A.7; Gaussian, Inc.: Pittsburgh, PA, 1998.
(56) Wesołowski, T. A. *J. Chem. Phys.* **1997**, *106*, 8516.
(57) Wesołowski, T. A.; Goursot, A.; Weber, J. *J. Chem. Phys.* **2001**, *115*, 4791.
(58) Wesołowski, T. A.; Weber, J. *Chem. Phys. Lett.* **1996**, *248*, 71.

(59) (a) St-Amant, A.; Salahub, D. R. *Chem. Phys. Lett*. **1990**, *169*, 387. (b) St-Amant, A. Ph.D. Thesis, University of Montreal, Montreal, Canada, 1992. (c) Casida, M. E.; Daul, C.; Goursot, A.; Koester, A.; Pettersson, L. G. M.; Proynov, E.; St-Amant, A.; Salahub, D. R., principal authors; Chretien, S.; Duarte, H.; Godbout, N.; Guan, J.; Jamorski, C.; Leboeuf, M.; Malkin, V.; Malkina, O.; Nyberg, M.; Pedocchi, L.; Sim, F.; Vela, A., contributing authors, *deMon-KS*, version 3.5; University of Montreal: Montreal, Canada, 1997. (d) Implementation of KSCED formalism by T. A. Wesołowski in deMon program: Wesołowski, T. A.; Weber, J. *Chem. Phys. Lett.* **1996**, *248*, 71.

(60) Lee, H.; Lee, C.; Parr, R. G. *Phys. Rev. A* **1991**, *44*, 768.

(61) Wesołowski, T. A.; Chermette, H.; Weber, J. *J. Chem. Phys.* **1996**, *105*, 9182.

(62) Godbout, N.; Salahub, D. R.; Andzelm, J.; Wimmer, E. *Can. J. Chem.* **1992**, *70*, 560.

(63) Simon, S.; Duran, M.; Dannenberg, J. J. *J. Chem. Phys.* **1996**, *105*, 11024.

(64) Salvador, P.; Paizs, B.; Duran, M.; Suhai, S. *J. Comput. Chem.* **2001**, *22*, 765.

(65) Vulliermet, N. Ph.D. Thesis, University of Geneva, Geneva, Switzerland, 2000.